Pol. J. Environ. Stud. Vol. 32, No. 4 (2023), 3437-3446
DOI: *10.15244/pjoes/163608* ONLINE PUBLICATION DATE: 2023-06-06

Original Research

Modelling of Selective Catalytic Reduction of NO_x with NH_3 over the Fe-Cu/ZSM-5 Catalyst

Hongquan Zhou[1, 2], Xueding Song[2], Dezhen Chen[1]*, Zhenzhen Guan[3]**

[1]Thermal and Environmental Engineering Institute, Tongji University, Shanghai 200092, China
[2]Shanghai Environmental Sanitation Engineering Design Institute Co.Ltd., Shanghai 200232, China
[3]College of Energy and Mechanical Engineering, Shanghai University of Electric Power, Shanghai 200090, China

Received: 20 February 2023
Accepted: 25 April 2023

Abstract

In this paper, a kinetic model was developed to simulate the reaction process of the Fe-Cu/zeolite Socony Mobil-5 (ZSM-5) catalyst for selective catalytic reduction of NO_x with NH_3 (NH_3-SCR). The global kinetic modeling accounted for various reactions occurring in SCR, including NH_3 adsorption/desorption, standard SCR, fast SCR, slow SCR, NH_3 oxidation, NO oxidation and N_2O formation reactions. The denitrification experiments were performed in a flow reactor with a feed stream, and the model could accurately predict the steady state conversion of NO at the reactor outlet. The results showed that the Fe-Cu/ZSM-5 catalyst exhibited an excellent catalytic activity, a high N_2 selectivity and an extended operating-temperature window across all temperatures ranging from 70 to 600ºC. By analyzing the influencing factors of the denitrification reaction, the results showed the temperature window shifted to lower temperatures with the gas hourly space velocity (GHSV), molar ratio of NH_3/NO (normalized stoichiometric ratio, NSR), molar ratio of NO_2/NO_x as well as NO inlet concentration, and the operating window could be broadened with an increase in the O_2 concentration; lower GHSVs promoted the N_2O formation. Due to ZSM-5 being rich in oxygen, the Fe-Cu/ZSM-5 catalyst exhibited high catalytic activity even without O_2. The research findings could provide insight into improving low temperature SCR reactivity of zeolite-based catalysts.

Keywords: low temperature selective catalytic reduction (LT SCR), Fe-Cu/ZSM-5 catalysts, zeolite, kinetic modeling

Introduction

The selective catalytic reduction (SCR) of NO_x with NH_3 is currently the most effective technology established for the abatement of NO_x emissions from stationary sources [1]. In the flue gas, NO_x (about 95% NO) react with O_2 and injected NH_3 according to the following equation: $4NO + 4NH_3 + O_2 \rightarrow 4N_2 + 6H_2O$. Commercial catalysts, in the form of honeycomb monoliths, are composed of an anatase TiO_2 carrier supporting the active components, namely, V_2O_5 and WO_3 (or MoO_3) for the flue gas at a temperature of 300 to 400ºC [2, 3].

However, due to the biological toxicity of V_2O_5 to humans and the environment, the narrow operation temperature window (300-400ºC), and the undesired

*e-mail: chendezhen@tongji.edu.cn
** e-mail: guanzzhen@163.com

oxidation of NH_3 to N_2O, their application to nonelectric plants is limited [4]. In order to develop efficient, non-toxic, economic and wide-temperature-window $deNO_x$ catalysts, metal-exchanged zeolite catalysts have received wide attention [5-12]. Jung et al. [13] studied the NO_x conversion on NH_3-SCR over the Cu-zeolite catalyst and V_2O_5-WO_3/TiO_2 catalyst, and found that the Cu-zeolite catalyst had a superior activity. Cho et al. [14] studied the reactivity of a commercial Fe-zeolite catalyst in the NH_3-SCR reactions for the aftertreatment of diesel exhausts and compared with a commercial V_2O_5-WO_3/TiO_2 catalyst, which indicated that the Fe-zeolite catalyst had a relatively high NO_x conversion efficiency. Colombo et al. [15] investigated the NH_3-SCR reactions over a commercial Cu-zeolite catalyst and a Fe-zeolite catalyst, suggesting that the Cu-zeolite catalyst was more active at lower temperatures, while the Fe-zeolite catalyst was highly active at higher temperatures. Among zeolite-based catalysts, Cu-ZSM-5 and Fe-ZSM-5 catalysts show good catalytic performance for SCR of NO_x with NH_3 [16]. Moreover, the NO_x conversion and N_2 selectivity of the Cu-exchanged ZSM-5 are higher than those of the Fe-exchanged ZSM-5 [17]. A single zeolite containing two cations, i.e., Cu and Fe are also attempted for increasing the NO_x conversion activities, and proved that the Cu-Fe/ZSM-5 catalyst shows higher NO_x conversion compared with Fe/ZSM-5 or Cu/ZSM-5 [18]. The combination of Fe and Cu doping over the zeolite catalyst usually show complementary advantages and synergistic effects [16, 19, 20]. Panahi et al. [21] found that the Cu/ZSM-5 nanocatalyst was the most promising catalyst, and the Fe-Cu/ZSM-5 bimetallic nanocatalyst had very high activities for NO conversion when adding different transition metals (Co, Mn, Cr and Fe) for the modification of Cu/ZSM-5. Previous studies also showed that the bimetallic catalyst comprising monolith coated with Fe- and Cu-zeolites achieved a high NO_x conversion over a wide range of temperatures [22-25].

In the previous work, the SCR-$deNO_x$ reaction over commercial Cu-zeolite and Fe-zeolite catalysts was studied under transient conditions in order to develop a dynamic kinetic model applicable to NO_x removal from the exhaust originating from diesel engine vehicles [26, 27]. However, an unsteady model of the SCR process for the binary Cu and Fe oxides based on zeolite had rarely been reported.

In order to investigate the dynamics of the SCR reaction over FeCu binary oxides, kinetic runs were performed over a powdered Fe-Cu/zeolite Socony Mobil-5 (ZSM-5) catalyst sample, and optimized with the experimental measurement data to study the performance of NH_3-SCR. The experiments were performed in a continuous flow reactor by continuously monitoring the species concentrations at the reactor outlet. In the light of the reactions occurring in SCR, the kinetic model was developed for various reactions, including NH_3 adsorption and desorption, standard SCR, fast SCR, slow SCR, NH_3 oxidation, NO oxidation as well as N_2O formation reactions. The main kinetic parameters were determined by calibrating the model to the reactor data. The optimized kinetic model could simulate the actual performance of the Fe-Cu/ZSM-5 catalyst such as NH_3 storage, NO_x conversion and N_2O formation. The improvement of the SCR process based on this kinetic model is of great significance to reduce NO_x and N_2O emissions simultaneously.

Material and Methods

Catalyst Preparation

The Fe-Cu/ZSM-5 catalyst samples were prepared by the sol-gel method, using ZSM-5 as the carrier and copper nitrate and iron nitrate as the precursors, which were all supplied by Shanghai Aladdin Biochemical Technology Co., Ltd. In the synthesis of the Fe-Cu/ZSM-5 catalyst, 0.005 mol of cupric nitrate trihydrate and 0.005 mol of iron (III) nitrate nonahydrate were initially added into 50 mL deionized water with stirring. Then, 0.015 mol of citric acid monohydrate (Sinopharm Chemical Reagent Co., Ltd.) was added into the mixture. After 1 h of mixing, 4.842 g of ZSM-5 was poured slowly into the mixture and anhydrous ethanol dripped into the mixture under continuous stirring to form transparent sol. The ZSM-5 loading was about 60 wt.%. Next, the obtained sol was heated at 80ºC overnight to convert into a xerogel and subsequently calcined in a muffle furnace at 500ºC for 4 h. Then, the sample was grounded into 60-100 mesh for activity testing.

Reactor Setup and Activity Testing

The denitrification performance of the catalyst samples was tested on a quartz tubular fixed-bed reactor (see Fig. 1) with an inner diameter of 85 mm and a catalyst length of 1 cm. The composition of the simulated gas was 120 ppm NO, 120 ppm NH_3, 6% O_2 with N_2 as a balance gas. The total flow of the gas was constant at 1 L/min and the corresponding gas hourly space velocity (GHSV) was 108 000 h^{-1}. The denitrification experiments were carried out in the temperature range of 70-412ºC with sufficient time for achieving steady-state operating points.

The Testo 350 flue gas analyzer was used to detect the NO_x concentration of the exit gas. The denitrification efficiency η and N_2 selectivity of the sample were calculated as follows:

$$\eta = \frac{[NO_x]_{in} - [NO_x]_{out}}{[NO_x]_{in}} \times 100\%,$$

$$N_2 \text{selectivity} = (1 - \frac{2[N_2O]_{out}}{[NO_x]_{in} + [NH_3]_{in} - [NO_x]_{out} - [NH_3]_{out}}) \times 100\%.$$

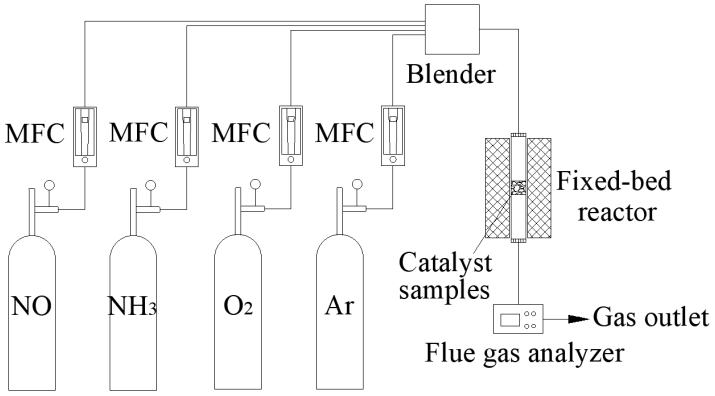

Fig. 1. Schematic diagram of experimental apparatus. MFC: mass flow controller.

Here, $[NO_x]_{in}$ and $[NH_3]_{in}$ respectively represented the reactor inlet volume concentrations of NO_x and NH_3; $[NO_x]_{out}$, $[NH_3]_{in}$ and $[N_2O]_{in}$ respectively represented the reactor outlet volume concentrations of NO_x, NH_3 and N_2O.

Model

Reactor Model

This reactor model reproduced the chemical reactions occurring on the catalyst during NH_3-SCR and aimed to simulate the chemical reactions occurring on a powdered catalyst. A one-dimensional isothermal homogeneous phase was modeled for analysis based on experimental data and individual primitive reactions, and some assumptions were made to optimize the computational time. Assuming that all channels were similar, the reactor model was simplified to a one-dimensional plug-flow reactor model.

The heat of reaction in the NH_3-SCR reaction was small, so the model was considered adiabatic. The dimensional parameters of the SCR catalyst were shown in Table 1.

Kinetic Model

The kinetics of reaction follows the Arrhenius law, and the reaction constants are described by the Arrhenius equation:

Table 1. Dimension parameters of the SCR catalyst.

Parameters	Value
Volume/cm^3	0.5671
Length/mm	10
Cell density/m^{-2}	0.25808
Wall thickness/mm	0.127
Washcoat thickness/mm	0.04

$$k = A\exp(-\frac{E_a}{RT})$$

where A is the pre-exponential factor of the reaction, E_a is the activation energy of the reaction, R is the gas constant, and T is the temperature of the reaction. The factors affecting the NH_3-SCR reaction were found to be mainly the pre-exponential factor and activation energy through literature research. Details on how to calibrate the pre-exponential factor and activation energy of chemical reactions could be described in subsequent sections.

The SCR kinetic model was mainly composed of mathematical control equations and chemical reaction mechanisms, and the mathematical control equations were mainly composed of momentum and energy conservation equations. This section focused on the chemical reaction mechanism of each primitive reaction, including the side reactions of NH_3-SCR. The main prevailing reactions were shown in Table 2.

Among them, R1 and R2 are the reactions of NH_3 adsorption and desorption, which have important effects on the NH_3 storage capacity and transient response

Table 2. Global reactions of the Fe-Cu/ZSM-5 catalyst.

Number	Reaction name	Reaction
R1	NH_3 adsorption	$NH_3+S\rightarrow NH_3(S)$
R2	NH_3 desorption	$NH_3(S)\rightarrow NH_3+S$
R3	Standard SCR	$4NH_3(S)+4NO+O_2\rightarrow 4N_2+6H_2O$
R4	Fast SCR	$4NH_3(S)+2NO+2NO_2\rightarrow 4N_2+6H_2O$
R5	Slow SCR	$8NH_3(s)+6NO_2\rightarrow 7N_2+12H_2O$
R6	NH_3 oxidation	$4NH_3(s)+3O_2\rightarrow 2N_2+6H_2O$
R7	NO oxidation	$2NO+O_2\rightarrow 2NO_2$
R8	N_2O formation	$2NH_3(S)+2NO_2\rightarrow N_2+N_2O+3H_2O$

characteristics of the Fe-Cu/ZSM-5 catalyst. R3 is the reaction of standard SCR, which occurs when the molar ratio of NO_2 and NO_x is less than 0.5, and the standard SCR reaction is the dominant reaction that determines the catalyst activity. R4 is a fast SCR reaction, which occurs when NO_2/NO_x = 0.5, and its reaction rate is about 17 times that of standard SCR when the reaction temperature is below 350ºC. R5 is a slow SCR reaction, which occurs when NO_2/NO_x >0.5, and the reaction rate declines because excess NO_2 not only lowers the denitration reaction rate but also promotes the formation of by-products like N_2O and NH_4NO_3. R6 is the oxidation of NH_3, which is an important side reaction for consuming NH_3 in NH_3-SCR. R7 and R8 are the oxidation of NO and the production of N_2O, respectively.

Reaction Model Parameter Optimization

According to the Arrhenius equation, the core parameters affecting the SCR catalytic reaction are the pre-exponential factor and the activation energy. The parameter that best reflects the catalyst activity is the denitrification efficiency. In this study, the genetic algorithm was used to optimize the pre-exponential factor and activation energy using the variance between the experimental data of denitrification efficiency and the simulated value as the objective function. The experimental and simulated values were fitted by adjusting several parameters in the model. The objective function was given by the following equation:

$$f = \frac{\int_0^{t_n} [C_{sim} - C_{exp}]^2}{t_n}$$

where f was the variance yields, C_{sim} was the simulation value, C_{exp} was the experimental value, and t_n was the time.

The parameters of the genetic algorithm were set as shown in Table 3.

Rate parameter estimates were obtained after the reaction kinetic optimization, in which the single site adsorption assumption was adopted in the Fe-based ZSM-5 catalyst and the dual-site adsorption assumption was adopted in the Cu-based ZSM-5 catalyst. The dynamic kinetic model was improved based on a mathematical model of the SCR monolith reactor, specifically adapted from Tronconi et al [28, 29]. The concentration of the species involved in reactions in Table 2 with temperature was solved by referring to standard numerical procedures [30].

Table 3. Parameters of the genetic algorithm.

Parameters	Value
Distribution for crossover probability	10
Distribution for mutation probability	10
Number of generations	20
Population size	50
Crossover probability	0.5
Mutation probability	0.05

Fig. 2 showed the fitted curves of the simulated values and the experimental values. From Fig. 2, it could be seen that for each temperature point of NO conversion, the absolute error between simulation and experimental data did not exceed 5 %. The simulated values of NO conversion at the catalyst outlet were close to the experimental values, which indicated that the optimized reaction kinetic parameters were consistent with the actual values.

Results and Discussion

Transient Adsorption and Desorption of NH_3

The adsorption and desorption of NH_3 is an important step in the NH_3-SCR reaction, which has a significant influence on the storage capacities of NH_3 on the catalyst surface and the transient response characteristics of deNO_x. The adsorption-desorption behavior of NH_3 over the Fe-Cu/ZSM-5 catalyst was investigated by temperature programmed desorption (TPD) modeling, which adopted Temkin-type kinetics to describe the NH_3 adsorption/desorption process over the Fe-Cu/ZSM-5 catalyst.

In a typical run, a feed containing 500 ppm NH_3 in Ar was introduced during the first 60 min at the initial adsorption temperature of 150ºC and GHSV of 108 000 h^{-1}. NH_3 uptake occurred during the induction period, and exhibited a dead time before growing up to 500 ppm. After achieving saturation, the NH_3 feed was shut off (t = 3600 s) and the outlet NH_3 concentration decreased monotonically with time due to the desorption of previously weakly adsorbed NH_3. Complete desorption of weakly absorbed NH_3 was achieved upon subsequent heating of the catalyst at 5400 s. The ramp rate was 10ºC/min to 600ºC. During the temperature ramp, a desorption peak was observed, at around 280ºC associated with the desorption of strongly adsorbed NH_3.

The temporal evolution of inlet and outlet NH_3 concentrations, as well as the catalyst temperature profile during an adsorption/desorption run at 150ºC with the subsequent TPD, was shown in Fig. 3. In this case, the NH_3 adsorption capacity and the activation energy for NH_3 desorption were estimated 196.62 μmol/gcat and 20.09 kcal/mol, respectively.

Effect of GHSV

GHSV is one of the key factors in the design of a catalytic system. Fig. 4 displayed the effect of the

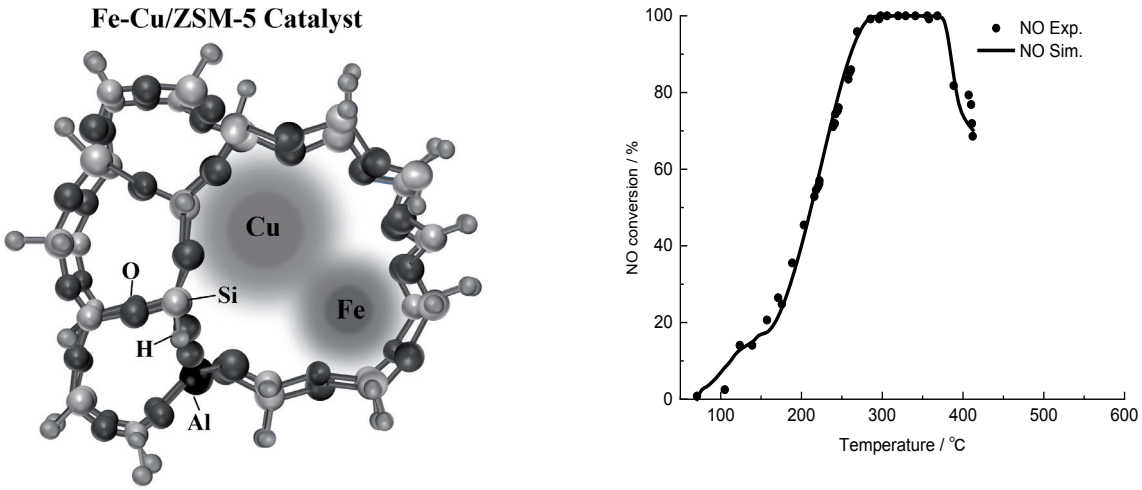

Fig. 2. NO conversion of experimental and simulated evolutions versus temperature. Reaction condition: 120 ppm NO, 120 ppm NH_3, 6% O_2 (balanced by N_2), GHSV = 108 000 h^{-1}.

GHSV on NO conversion and N_2O formation. During the modeling, the composition of the simulated gas was consistent with the experiment, except that GHSV varied from 50 000 to 300 000 h^{-1}. The NO conversion as well as N_2O formation was simulated at different GHSVs.

As shown in Fig. 4a), the conversion of NO was high when the GHSV was in the range of 50 000 -300 000 h^{-1}, due to the fact that there was enough time for reactions to occur on the catalyst surface. However, when the GHSV increased from 100 000 to 300 000 h^{-1}, the peak efficiency decreased slightly from 99.98 to 98.36 %. The reason may be that the higher GHSV was associated with a shorter residence time in the reaction zone, resulting in insufficient contact between the reactant gas and the active sites on the catalyst surface, leading to a slight decrease in NO conversion at high GHSVs. In addition, the temperature window slightly shifted to lower temperatures with

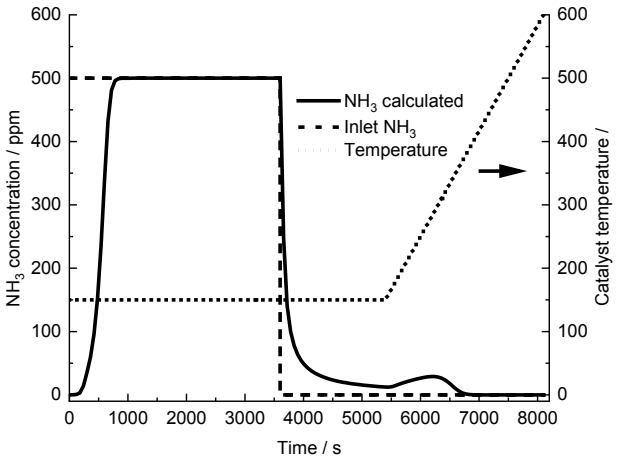

Fig. 3. NH_3 adsorption-desorption over Fe-Cu/ZSM-5 (solid line: kinetic fit; dashed line: inlet NH_3 concentration; dotted line: catalyst temperature).

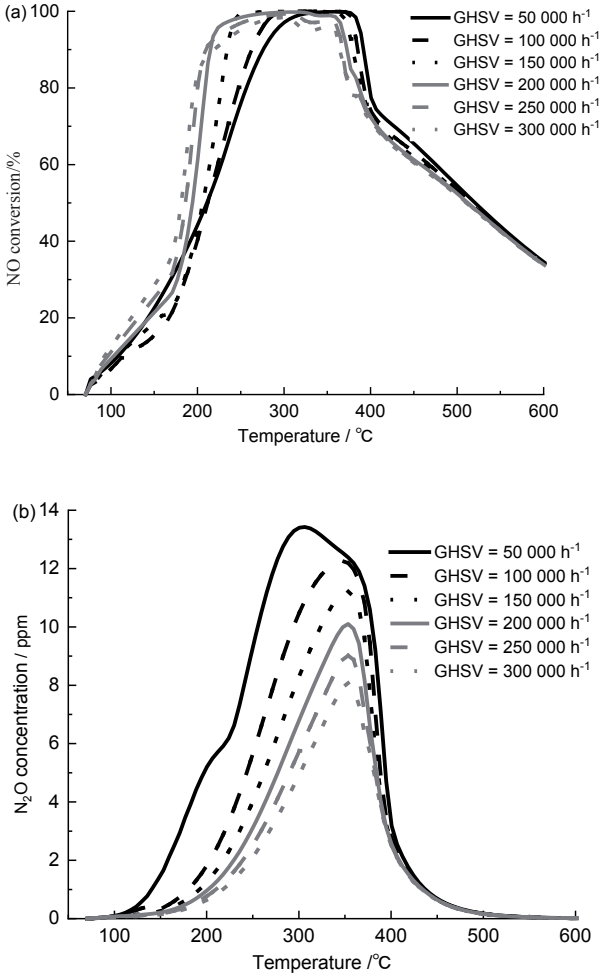

Fig. 4. a) NO conversion and b) N_2O formation at different GHSVs. Reaction conditions: [NO] = [NH_3] = 120 ppm, [O_2] = 6 %, N_2 balance.

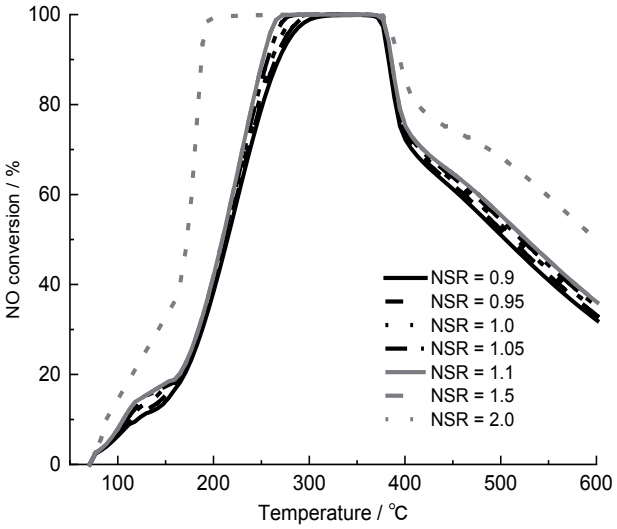

Fig. 5. The effect of NSR on the conversion of NO. Reaction conditions: [NO] = 120 ppm, [O_2] = 6 %, N_2 balance, GHSV = 108 000 h^{-1}.

the GHSV, since the NO light-off temperature could be lowered via a high mixing efficiency of adsorbed NH_3 species with gas-phase or weakly adsorbed NO species.

Fig. 4b) showed the N_2O formation at different GHSVs. It could be seen that the effect of the GHSV on N_2O production was significant. Different from NO reduction curves, the temperature window for N_2O formation shifted to high temperatures and the N_2O concentration decreased with an increase in the GHSV over the whole investigated temperature range. Since the N_2O formation mainly originated from the oxidation of adsorbed NH_3, the longer residence time corresponding to the lower GHSVs was conducive to side reactions to take place, such as N_2O production.

The results in Fig. 4 suggested that the GHSV mainly affected the adsorption of NH_3 as well as the mixture of the reactant species, and thus affected the processes of NO reduction and N_2O formation.

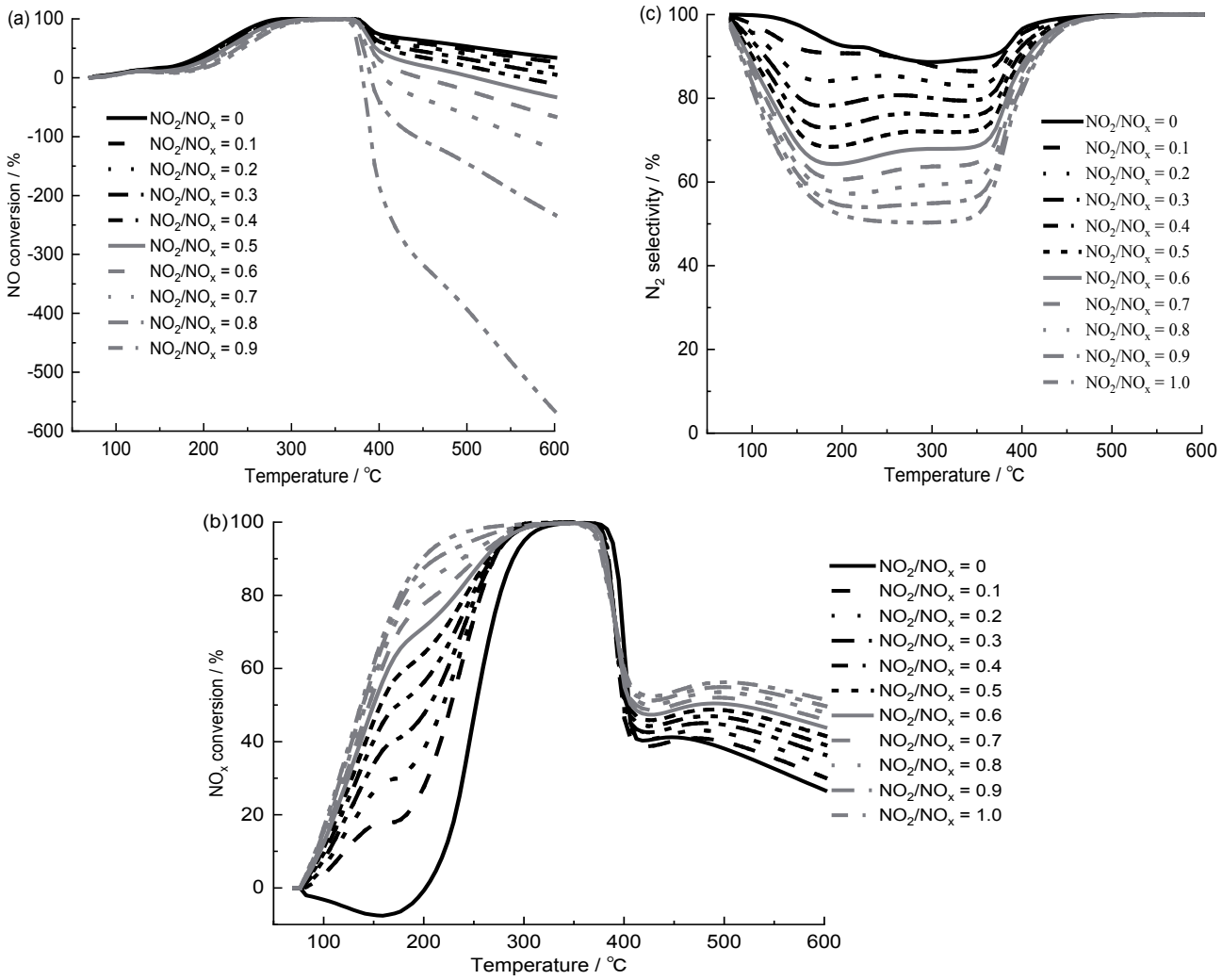

Fig. 6. Effect of NO_2/NO_x feed ratio on de-NO_x efficiency (a,b) and N_2 selectivity c). Reaction conditions: [NO_x] = 120 ppm, [O_2] = 6%, N_2 balance, GHSV = 108 000 h^{-1}.

Effect of NSR

Considerable studies have shown that the ammonia to nitrogen ratio (normalized stoichiometric ratio, NSR) has a significant impact on the catalyst activity. We simulated the effect of NSR on deNO$_x$ activity with 120 ppm NO, 6 % O_2, GHSV of 108 000 h^{-1}, as well as NSR from 0.9 to 2.0. Fig. 4 showed the conversion of NO at different NSRs.

The results in Fig. 5 showed that the NO conversion increased and the operating window broadened with an increase in NSR, which was due to the fact that more NH_3 dosing accelerated the standard SCR reaction. However, the excess NH_3 may be oxidized by side reactions. Hence, the reaction was suggested carrying out at NSR from 0.9 to 1.5.

Effect of the Molar Ratio of NO_2/NO_x

In practical applications, the real gas composition is actually complex and usually contains some amount of NO_2. The relevant literature demonstrated that the proportion of NO_2 in NO_x had a large impact on the deNO$_x$ reaction. The reason for this is that different NO_2/NO_x feed ratios can lead to different SCR reactions, such as when NO_2/NO_x = 0.5, a fast SCR reaction takes place, which is significantly faster than the standard SCR. The model predicted the effect of NO_2/NO_x feed ratios on the NOx conversion and N_2 selectivity, shown in Fig. 6. In all cases, the feed mixture contained 120 ppm NO_x and 6% O_2 with N_2 as a balance gas. The GHSV was set to 108 000 h^{-1}. The NO_2/NO_x feed ratios were varied in the following levels: 0, 0.1, 0.2, 0.3, 0.4, 0.5, 0.6, 0.7, 0.8, 0.9 and 1.0.

From Fig. 6a) and b), we could observe that the enhancement in the NOx removal by NO_2 was not nearly as significant. The Fe-Cu/ZSM-5 catalyst had a very high NO reduction efficiency even for non-NO_2 feeding. In contrast to the NO reduction curve, the temperature window broadened and the NO_x removal efficiency nearly increased with the increase of the NO_2/NO_x feed ratio expect the temperatures ranging from 270 to 460ºC for NO_x reduction. Thus, the NO_x reduction activity at NO_2/NO_x = 0.5 was not nearly so dramatic.

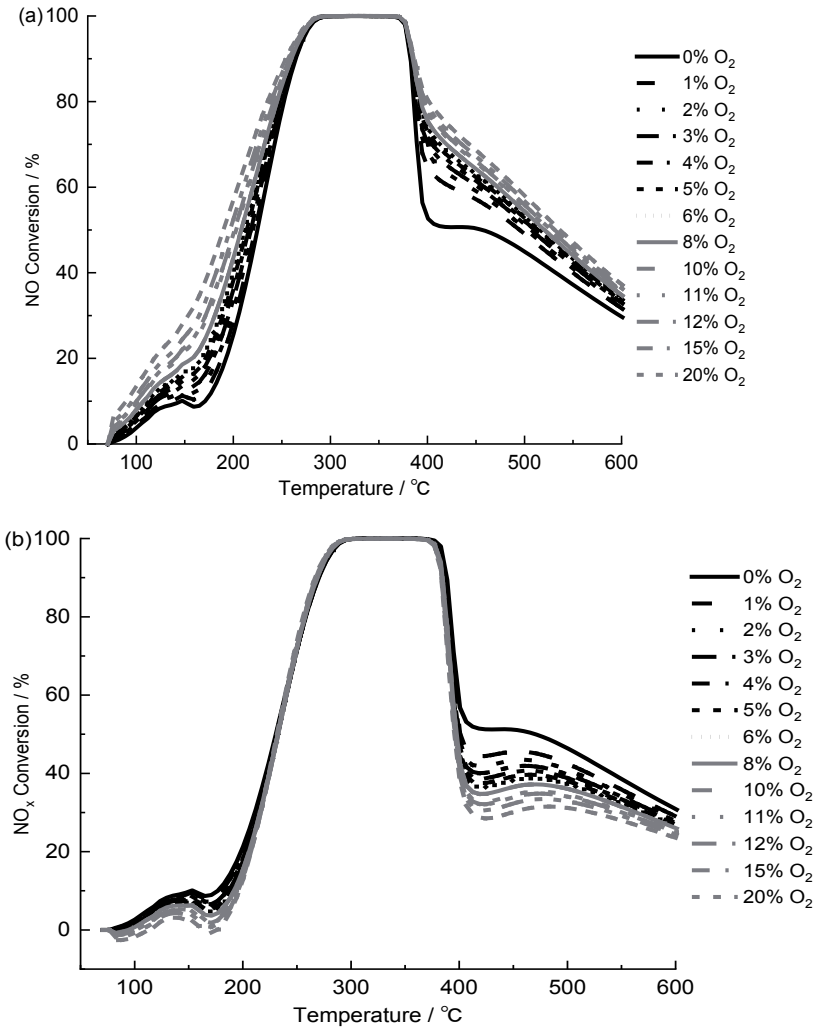

Fig. 7. Effect of the O_2 concentration on deNO$_x$ efficiency. Reaction conditions: [NO] = [NH_3] = 120 ppm, N_2 balance, GHSV = 108 000 h^{-1}.

Besides, an important goal of NH_3-SCR is to selectively convert NO_x to N_2 to the maximum extent. Fig. 6c) showed the predicted influence of the ratio of NO_2 in the feed on the N_2 product yield. The model predictions exhibited a noticeable decline in the N_2 selectivity with increasing the molar ratio of NO_2/NO_x, which had shown similar catalytic characterization with the Cu-chabazite (CHA) catalyst [26]. From Fig. 6, it was evident that when NO_2/NO_x = 0, the NO removal efficiency was the highest and the N_2 selectivity was the best. This was because when the ratio of NO_2 in NO_x was greater than 0.5, the generation of by-products such as N_2O would occur.

Therefore, in view of the NO reduction and selectivity towards N_2, the feed without NO_2 gave the optimal NO removal performance on the Fe-Cu/ZSM-5 catalyst. It demonstrated that the Fe-Cu/ZSM-5 catalyst was more likely to be suitable for NO_x abatement than the V/Ti-based catalyst in the actual NO-dominated flue gas.

Effect of the O_2 Concentration

O_2 is an important component in an actual combustion flue gas. Fig. 7 depicted the effect of the O_2 concentration on deNO_x activity at various temperatures (70-600ºC) as follows: 120 ppm NO, 120 ppm NH_3, 0-20 % O_2, balance N_2 and GHSV = 108 000 h^{-1}.

The results of previous studies showed that the catalyst surface with molecular sieve as the carrier was rich in oxygen vacancies, which could provide sufficient chemisorbed oxygen and lattice oxygen for the denitrification reaction [31]. It was observed from Fig. 7a) that the window widened, and the NO removal efficiency increased with the increase of O_2 concentration, showing a plateau in a temperature range from 280ºC up to 377ºC for all concentration ranges of O_2.

The data from Fig. 7. exhibited that different from the selective non-catalytic reduction (SNCR) reaction which did not occur in the absence of O_2, the Fe-Cu/ZSM-5 catalyst showed very high NO_x removal efficiency even without O_2. It may be concluded that ZSM-5 could catalyze the SCR reaction by providing enough oxygen.

Effect of the NO Initial Concentration

The NO inlet concentration has a great influence on the SCR denitrification reaction. We calculated the conversion efficiency of the catalyst when the NO concentration was 120 ppm, 200 ppm, 300 ppm, 500 ppm, 800 ppm and 1000 ppm. The simulation results were shown in Fig. 8.

The kinetic calculation results showed that the denitrification efficiency exhibited an increasing trend when the inlet NO concentration increased except for temperatures at about 306-388ºC. The data in Fig. 8

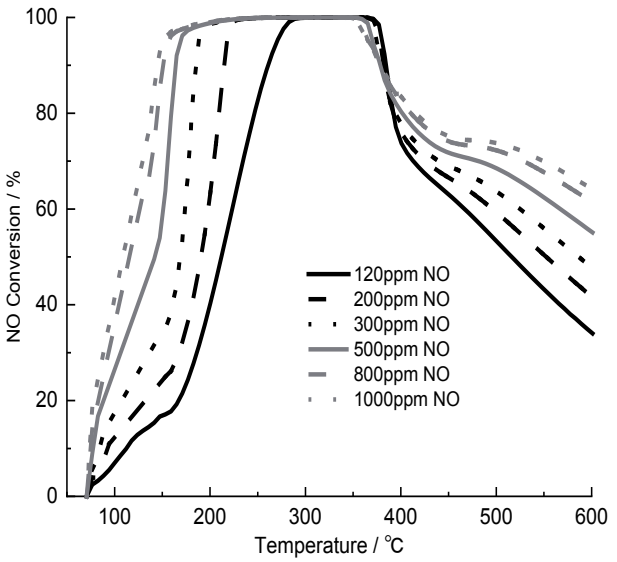

Fig. 8. Effect of the NO initial concentration on denitrification efficiency. Reaction conditions: [NO] = [NH_3], [O_2] = 6%, N_2 balance, GHSV = 108 000 h^{-1}.

demonstrated that the NO light-off temperatures could be lowered, and the windows could be broadened as the NO initial concentration increased. When the inlet NO_x concentration was increased to 1000 ppm, the catalyst was active for NO reduction at lower temperatures and lighted off below 120ºC, achieving a plateau of the denitrification efficiency holding over 97% NO conversion at temperatures ranging from 160 to 360ºC. Thus, the higher inlet NO concentration improved LT SCR activity.

Conclusions

We performed global kinetic modeling over the Fe-Cu/ZSM-5 catalyst. The kinetic model considered NH_3 adsorption-desorption, standard SCR, fast SCR, NO_2 SCR, NH_3 oxidation, NO oxidation and N_2O generation. In the study, the effects of the GHSV, NSR, molar ratio of NO_2/NOx, O_2 concentration and NO initial concentration were investigated.

The Fe-Cu/ZSM-5 catalyst exhibited a boosted activity, a high N_2 selectivity and a wide operating temperature range from 70 to 600ºC. The results showed that the GHSV mainly affected the adsorption of NH_3 as well as other reactant species, and thus affected the processes of NO reduction and N_2O formation. The NO conversion increased and the operating window broadened with an increase in NSR, which was due to the fact that more NH_3 dosing speeded up the standard SCR reaction. However, the excess NH_3 may be oxidized by side reactions. In view of the NO reduction and N_2 selectivity, the feed without NO_2 gave the best NO removal efficiency on the Fe-Cu/ZSM-5 catalyst covering all temperatures between 70 and 600ºC.

Moreover, the Fe-Cu/ZSM-5 catalyst also showed very high NO_x removal performance even without O_2. It may be concluded that ZSM-5 could catalyze the SCR reaction by providing sufficient oxygen. The higher NO initial concentration improved low-temperature SCR activity. In summary, the Fe-Cu/ZSM-5 catalyst was suggested to be used under operating conditions of GHSVs of ≤300 000 h^{-1}, NSR from 0.9 to 1.5, NO_2/NO_x feed ratios varying from 0 to 1.0 and 0-20 % O_2. The findings revealed that the Fe-Cu/ZSM-5 catalyst had immense potential and was well suited for LT NH_3-SCR operation without O_2 or with excess O_2 in a wide NO initial concentration range over the temperature window between 70 and 600ºC.

Acknowledgments

The Authors are grateful for the financial support received from National Natural Science Foundation of China (Granted No. 51776141).

Conflict of Interest

The authors declare no conflict of interest.

References

1. FAN Y., ZHANG J., YANG L., LU M., YING T., DENG B., DAI W., LUO X., ZOU J., LUO S. Enhancing SO_2-shielding effect and Lewis acid sites for high efficiency in low-temperature SCR of NO with NH_3: Reinforced electron-deficient extent of Fe^{3+} enabled by Ti^{4+} in Fe_2O_3. Sep. Purif. Technol. **311**, 123272, **2023**.
2. LEE G., YE B., LEE M., CHUN S., JEONG B., KIM H., JAE J., KIM T. Selective catalytic reduction of NO_x by NH_3 over V_2O_5-WO_3 supported by titanium isopropoxide (TTIP)-treated TiO_2. J. Ind. Eng. Chem. **109**, 422, **2022**.
3. ZHAO S., PENG J., GE R., YANG K., WU S., Qian Y., XU T., GAO J., CHEN Y., SUN Z. Poisoning and regeneration of commercial V_2O_5-WO_3/TiO_2 selective catalytic reduction (SCR) catalyst in coal-fired power plants. Process Saf. Environ. Prot. **168**, 971, **2022**.
4. JIA Y., ZHENG R., YUAN J., ZHANG X., WANG R., GU M., ZHANG S., CHEN Y., GUO L. Promoting catalytic performance by balancing acid and redox sites on Mn_3O_4–$Mn_2P_2O_7$/TiO_2 for selective catalytic reduction of NO by NH_3 at low temperature. Mol Catal. **536**, 112913, **2023**.
5. ZHANG W., CHEN J., GUO L., ZHENG W., WANG G.., ZHENG S., WU X. Research progress on NH_3-SCR mechanism of metal-supported zeolite catalysts. J. Fuel Chem. Techno. **49**(9), 1294, **2021**.
6. CHEN L., REN S., LIU L., SU B., YANG J., CHEN Z., WANG M., LIU Q. Catalytic performance over Mn-Ce catalysts for NH_3-SCR of NO at low temperature: Different zeolite supports. J. Environ. Chem. Eng. **10**(2), 107167, **2022**.
7. SHI Z., PENG Q., E J., XIE B., WEI J., YIN R., FU G. Mechanism, performance and modification methods for NH3-SCR catalysts: A review. Fuel. **331**, 125885, **2023**.
8. CHENG H., TANG X., YI H., PAN R., ZHANG J., GAO F., YU Q. Application progress of small-pore zeolites in purifying NO_x from motor vehicle exhaust. Chem. Eng. J. **449**, 137795, **2022**.
9. KUMAR M.S., ALPHIN M.S., KUMAR P.S., RAJA S. A review on zeolite catalyst for deNO_x performance in ammonia-selective catalytic reduction. Fuel. **334,** 126828, **2023**.
10. GOWRAM I., BEULAH M. Experimental and analytical study of high-strength concrete containing natural zeolite and additives. Civil Eng. J. **8**, 10, **2022**.
11. YANDRI Y., ROPINGI H., SUHARTATI T., HENDRI J., IRAWAN B., HADI S. The effect of zeolite/chitosan hybrid matrix for thermal-stabilization enhancement on the immobilization of Aspergillus fumigatus α-amylase. Emerg. Sci. J. **6**, 3, **2022**.
12. AKHTAR J.N., KHAN R.A., KHAN R.A., AKHTAR M.N., NEJEM J.K. Influence of natural zeolite and mineral additive on bacterial self-healing concrete: A review. Civil Eng. J. **8**, 5, **2022**.
13. JUNG Y., SHIN Y.J., PYO Y.D., CHO C.P., JANG J., KIM G. NO_x and N_2O emissions over a Urea-SCR system containing both V_2O_5-WO_3/TiO_2 and Cu-zeolite catalysts in a diesel engine. Chem. Eng. J. **326**, 853, **2017**.
14. CHO C.P., PYO Y.D., JANG J.Y., KIM G.C., SHIN Y.J. NO_x reduction and N_2O emissions in a diesel engine exhaust using Fe-zeolite and vanadium based SCR catalysts. Appl. Therm. Eng. **110**, 18, **2017**.
15. COLOMBO M., NOVA I., TRONCONI E. A comparative study of the NH_3-SCR reactions over a Cu-zeolite and a Fe-zeolite catalyst. Catal. Today. **151**(3-4), 223, **2010**.
16. ZHANG T., LIU J., WANG D., Zhao Z., WEI Y., CHENG K., JIANG G., DUAN A. Selective catalytic reduction of NO with NH_3 over HZSM-5-supported Fe–Cu nanocomposite catalysts: The Fe–Cu bimetallic effect. Appl. Catal. B-Environ. **148-149**, 520, **2014**.
17. LIU Y., HAROLD M.P., LUSS D. Coupled NOx storage and reduction and selective catalytic reduction using dual-layer monolithic catalysts. Appl. Catal. B-Environ. **121-122**, 239, **2012**.
18. SULTANA A., SASAKI M., SUZUKI K., HAMADA H. Tuning the NO_x conversion of Cu-Fe/ZSM-5 catalyst in NH_3-SCR. Catal. Commun. **41**, 21, **2013**.
19. WU G., LIU S., CHEN Z., YU Q., CHU Y., XIAO H. PENG H., FANG D., DENG S., CHEN Y. Promotion effect of alkaline leaching on the catalytic performance over Cu/Fe-SSZ-13 catalyst for selective catalytic reduction of NO_x with NH_3. J. Taiwan Inst. Chem. E. **134,** 104355, **2022**.
20. WANG X., SUN Y., HAN F., ZHAO Y. Effect of Fe addition on the structure and SCR reactivity of one-pot synthesized Cu-SSZ-13. J. Environ. Chem. Eng. **10,** 107888, **2022**.
21. PANAHI P.N., SALARI D., NIAEI A., MOUSAVI S.M. NO reduction over nanostructure M-Cu/ZSM-5 (M: Cr, Mn, Co and Fe) bimetallic catalysts and optimization of catalyst preparation by RSM. J. Ind. Eng. Chem. **19,** 1793, **2013**.
22. METKAR P.S., HAROLD M.P., BALAKOTAIAH V. Selective catalytic reduction of NO_x on combined Fe- and Cu-zeolite monolithic catalysts: Sequential and dual layer configurations. Appl. Catal. B-Environ. **111-112**, 67, **2012**.
23. METKAR P.S., BALAKOTAIAH V., HAROLD M.P. Experimental study of mass transfer limitations in Fe- and Cu-zeolite-based NH_3-SCR monolithic catalysts. Chem. Eng. Sci. **66**, 5192, **2011**.

24. JOUINI H., MEJRI I., PETITTO C., MARTINEZ-ORTIGOSA J., VIDAL-MOYA A., MHAMDI M., BLASCO T., DELAHAY G. Characterization and NH_3-SCR reactivity of Cu-Fe-ZSM-5 catalysts prepared by solid state ion exchange: The metal exchange order effect. Micropor. Mesopor. Mat. **260,** 217, **2018**.
25. YUAN E., LI M., YANG M., HUANG X., ZHANG K., HAN W., TANG Z., LIU Z. Encapsulation of ultra-small Cu–Fe into ZSM-5 zeolites for NH_3-SCR with broad reaction-temperature ranges. Micropor. Mesopor. Mat. **331,** 111675, **2022**.
26. METKAR P.S., HAROLD M.P., BALAKOTAIAH V. Experimental and kinetic modeling study of NH_3-SCR of NO_x on Fe-ZSM-5, Cu-chabazite and combined Fe- and Cu-zeolite monolithic catalysts. Chem. Eng. Sci. **87,** 51, **2013**.
27. LI S., ZHANG C., ZHOU A., LI Y., YIN P., MU C., XU J. Experimental and kinetic modeling study for N_2O formation of NH_3-SCR over commercial Cu-zeolite catalyst. Adv. Mech. Eng. **13** (4), 1, **2021**.
28. LIETTI L., NOVA I., CAMURRI S., TRONCONI E., FORZATTI P. Dynamics of the SCR-DeNO_x reaction by the transient-response method. AIChE J. **43** (10), 2559, **1997**.
29. TRONCONI E., CAVANNA A., FORZATTI P. Unsteady analysis of NO reduction over selective catalytic reduction-De-NO_x monolith catalysts. Ind. Eng. Chem. Res. **37**, 2341, **1998**.
30. HINDMARSH A.C. Toward a systematized collection of ODE solvers. 10th international mathematics and computers simulation congress on systems simulation and scientific computation, Montreal, Canada, 9 Aug **1982**.
31. HAO R., QIAN Z., YANG X., LUO M., FENG X., QIAO W., ZHAO Y., YUAN B. Enhanced removal of elemental mercury using MnO_2-modified molecular sieve under microwave irradiation. Chem. Eng. J. **450**, 137997, **2022**.